Sensor shapes and weak modes of the ATLAS Inner Detector track-based alignment

JULIAN WOLLRATH [1]

On behalf of the ATLAS Collaboration,
Physikalisches Institut
Albert-Ludwigs-Universität Freiburg, Germany

ABSTRACT

The alignment of the ATLAS Inner Detector is performed with a track-based algorithm. The aim of the detector alignment is to provide an accurate description of the detector geometry such that track parameters are accurately determined and bias free. The detector alignment is validated and improved by studying resonant decays (J/ψ and Z to $\mu^+\mu^-$). The detailed study of these resonances (together with the properties of the tracks of their decay products) allows to detect and correct for alignment weak modes such as detector curls and radial deformations that may bias the momentum and/or the impact parameter measurements. Here, radial distortions were investigated. Furthermore, a new analysis with a detailed scrutiny of the track-to-hit residuals allowed to study the deformation shape of the Pixel and IBL modules. The sensor distortion can result in track-to-hit residual biases of up to $10\,\mu m$ within a given module. The shape of the IBL modules was parametrised with Bernstein-Bézier functions and used to correct the hit position in the track fitting procedure.

PRESENTED AT

Connecting the Dots and Workshop on Intelligent Trackers (CTD/WIT 2019)
Instituto de Física Corpuscular (IFIC), Valencia, Spain
April 2-5, 2019

1 Introduction

Precision measurements such as that of the W boson mass [1] at the ATLAS experiment [2] require a precise determination of the absolute momentum scale of charged particles measured by the ATLAS Inner Detector (ID). Measurements of track momenta by the ID can be affected by several sources of biases, one of them being residual geometric deformations of the ID prevailing after its alignment, which can be either real geometrical deformations or ill-defined alignment solutions. Here, new work on the assessment of radial distortions with a layer inflation model is described.

The alignment and the quality of the reconstructed tracks can also be influenced by imprecise knowledge of the detector components. The extraction of the shape of ATLAS Insertable B-Layer (IBL) sensors from track-to-hit residuals is also described here.

2 Inner detector alignment

The actual geometry of the detector differs from its nominal geometry and is determined by a track-based alignment algorithm which is based on minimising track-to-hit residuals with the least square method [3]. The alignment parameters are determined iteratively and the alignment is performed on different hierarchical levels, where either whole structures such as the different layers or single modules are aligned. The alignment of different substructures or modules can introduce systematic biases which can be assessed by reconstructing invariant masses of particles decaying into a pair of muons, i.e. $J/\psi \to \mu^+\mu^-$ and $Z \to \mu^+\mu^-$.

3 Radial distortions

The transverse momentum of a charged particle emerging from the centre of a cylindrical detector satisfies the relation

$$p_\mathrm{T} \sim qB\frac{R_0^2}{8s}, \tag{1}$$

with particle charge q, uniform magnetic field B, detector radius R_0 and sagitta s of the trajectory.

A geometrical deformation that alters the detector radius to $\tilde{R}_0 = R_0 + \delta R$ is called a radial distortion and is depicted in figure 1. Radial distortions were previously studied in ATL-PHYS-PUB-2018-003 [4], the present work focuses on their dependence on the azimuth ϕ of the ID. It is assumed that the transverse and longitudinal momentum (p_T and p_z) of the tracks get changed to

$$\tilde{p}_\mathrm{T} = p_\mathrm{T}\left(1 + \frac{\delta R}{R_0}\right) \tag{2}$$

and analogously for p_z, while the incident angle θ of the tracks stay invariant. Given that $p_{\mathrm{T},1/2}$ and $\eta_{1/2}$ denote transverse momentum and pseudorapidity of the respective, assumed to be massless, decay particle, the mass m of a particle undergoing a two-body decay can be calculated as

$$m^2 = 2p_{\mathrm{T},1}p_{\mathrm{T},2}\big(\cosh\left(\eta_1 - \eta_2\right) - \cos\Delta\phi\big). \tag{3}$$

Hence, a radial distortion will change the measured mass to

$$\tilde{m} = m\left(1 + \frac{\delta R}{R_0}\right). \tag{4}$$

To assess the magnitude of this bias, the peak of the distribution of reconstructed di-muon masses m_fit was compared to the peak of the distribution of the di-muon masses in Monte-Carlo simulation m_MC. The ratio

$$\frac{\delta m}{m_\mathrm{MC}} = \frac{m_\mathrm{fit} - m_\mathrm{MC}}{m_\mathrm{MC}} \tag{5}$$
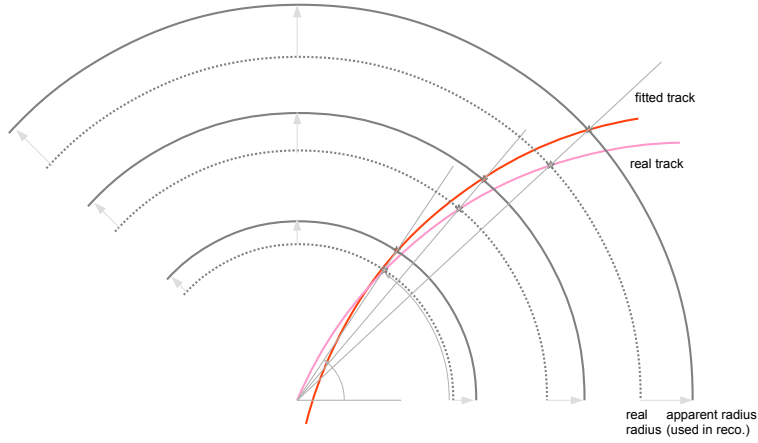
Figure 1: Sketch of a radial deformation: the real radii of the layers are shown as dotted lines, while the apparent layer radii are shown as solid lines. The inflation of the radius leads to a track-to-hit residual and a change in track curvature, which changes the momentum measurement.
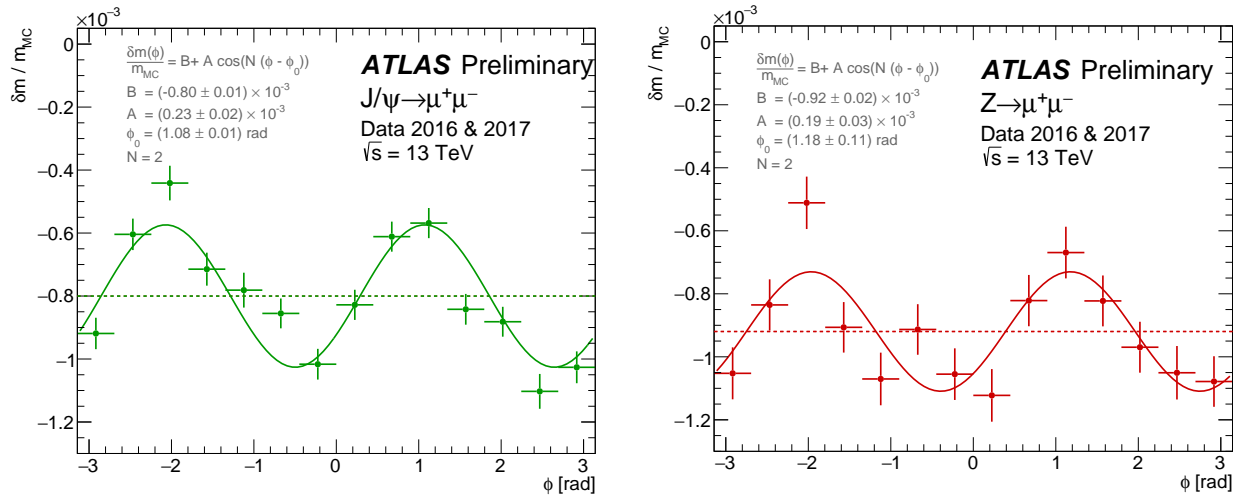

Figure 2: The reconstruction of invariant masses for $J/\psi \to \mu^+\mu^-$ (left) and $Z \to \mu^+\mu^-$ (right) points to the presence of a ϕ-dependent radial distortion.
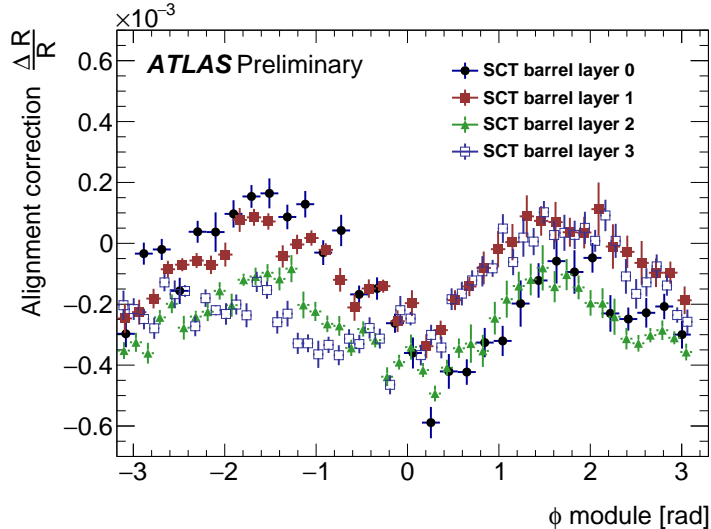
Figure 3: Radial distortions for the four SCT barrel layers. The modulation with respect to ϕ is compatible with an elliptical deformation with the minor axis in the horizontal plane and difference between major and minor axis of $\sim 100\,\mu\text{m}$.

which relates to a radial distortion was plotted against ϕ as shown in figure 2. The data points at the presence of a ϕ-dependent radial distortion, which could be observed in both $J/\psi \to \mu^+\mu^-$ and $Z \to \mu^+\mu^-$.

Radial distortions were also evaluated for the four barrel layers of the silicon strip detector (SCT) [5]. For these layers a radial distortion was also observed as shown in figure 3. These ϕ-dependent radial distortions are compatible with an elliptical deformation of the SCT layers with the minor axis of the deformation being in the horizontal plane and a difference between minor and major axis of $\sim 100\,\mu\text{m}$.

4 Insertable B-Layer sensor shape

The IBL [6], which was installed in 2014, consists of 14 staves. From one end to the other each of these is equipped with four 3D modules, twelve planar modules and again four 3D modules; all of these modules are silicon pixel modules. While the shapes of the modules of the original pixel detector were measured in a campaign in 2006 before they were installed into the experiment and hence their shape is taken into account when reconstructing tracks, no such measurement was done for the IBL modules; therefore they are assumed to be flat in track reconstruction. Whether this assumption holds can be evaluated by splitting the modules into small cells and calculating the average track-to-hit residual in these cells. These intra-module track-to-hit residuals of the IBL planar modules were evaluated for data from one long LHC fill taken on 9th to 10th November 2017 containing $\sim 9 \times 10^5$ IBL hits. This was done by rerunning the track reconstruction and performing one iteration of alignment for the IBL and pixel modules as is shown on the left hand side of figure 4. While the average track-to-hit residual per module is $\sim 0\,\mu\text{m}$, a clear intra-module structure, which is similar for all the modules, could be observed. This means that the IBL modules cannot assumed to be flat but instead have a shape in local-z; this shape can be extracted from the track-to-hit residuals and the track parameters. For this shape extraction a second, larger statistics data sample from late 2017 containing $\sim 2 \times 10^9$ tracks was used. Since the resolution of the detectors is finer in local-x than in local-y, the z-value for each track with an IBL hit was calculated as

$$z' = x_{\text{residual}} \cot \phi'. \tag{6}$$

The sensors were than split into 21×21 cells and the local-z value of each cell $\mathfrak{P}_{i,j}$ was calculated as the weighted mean of the z' values in the cell. To get a smooth approximation of the sensor surface this
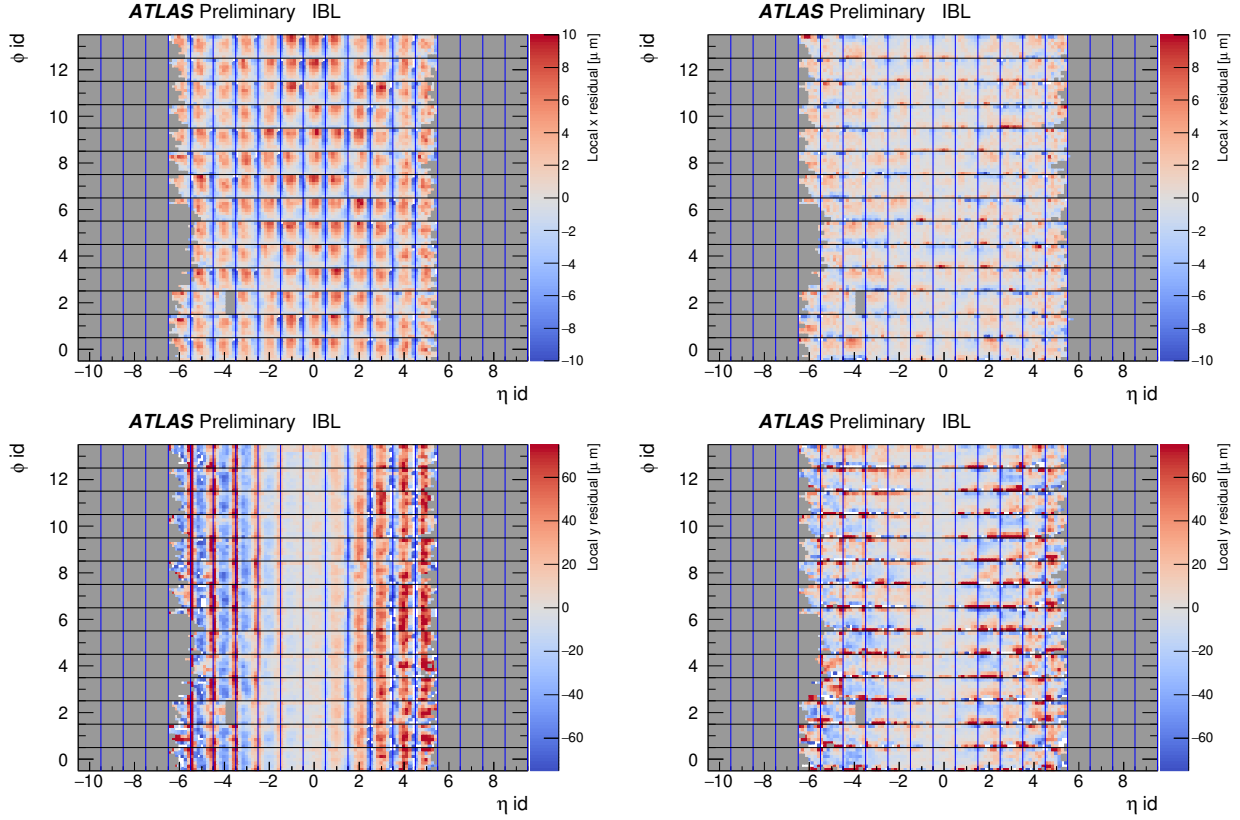
Figure 4: Intra-module local-x (top) and local-y (bottom) residuals for the IBL. On the left, IBL modules are assumed to be flat, while on the right shape corrections are taken into account. Taking the module shape into account reduces the intra-module residuals.

extracted shape was subsequently interpolated with a two-dimensional Bernstein-Bézier function as defined in equation (7) with the Bernstein basis polynomials defined in equation (8).

$$\mathfrak{r}(u,v) = \sum_{i=0}^{n} \sum_{j=0}^{m} B_{i,n}(u) B_{j,m}(v) \mathfrak{P}_{i,j} \,, \quad 0 \le u, v \le 1 \tag{7}$$

$$B_{i,n} = \binom{n}{i} t^i (1-t)^{n-i} \,, \quad 0 \le t \le 1 \quad (i = 0, 1, \ldots, n) \tag{8}$$

Utilising the data sample with a huge number of tracks, the shape of the planar IBL modules was measured. This shape and its interpolation for the IBL module with ϕ-ID 10 and η-ID 0 is shown on the left hand side of figure 5 and the difference between measured shape and interpolation is shown on the right hand side of figure 5; for most of the sensor, the deviation between measurement and interpolation is in the $\pm 2 \, \mu m$ range.

Over most of the modules, the sensor bends in the $\pm 20 \, \mu m$ range. A clear trend towards large negative values of the bending is observed for smaller x, which might be due to stress of a kapton flex that is attached to the module on that side.

To evaluate the impact of including the shape information for the IBL in the reconstruction, one iteration of alignment of the IBL and pixel modules was performed for the same LHC fill as before but this time taking the sensor shape into account. The intra-module track-to-hit residuals were evaluated as shown on the right hand side of figure 4. A clear improvement could be observed in the intra-module local-x and local-y residuals with the structure in the local-x residuals being mostly removed.
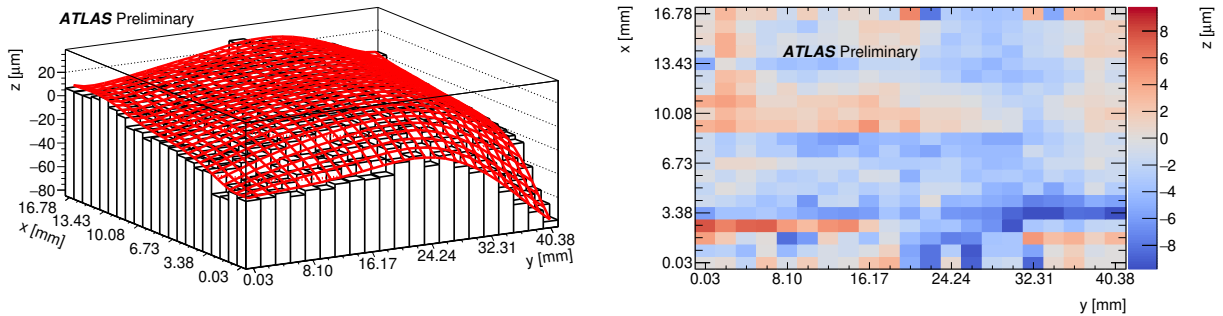
4

Figure 5: The shape of the IBL module with ϕ-ID 10 and η-ID 0 was extracted from track-to-hit residuals (left, black) and interpolated with a Bernstein-Bézier function (left, red). The difference between the shape extraction (black) and the interpolation (red) is shown on the right.

5 Conclusions

Radial distortions of the ATLAS Inner Detector were studied with a layer inflation model. The reconstruction of invariant masses point to the presence of a ϕ-dependent radial distortion. Furthermore the SCT barrel layers show a ϕ-dependent radial distortion compatible with an elliptical deformation. Having assessed these distortions, the knowledge about them could be included into the alignment procedure as an additional constraint and help in improving the ID alignment.

The shape of IBL sensors was extracted from track-to-hit residuals. A clear deviation from the flat sensor hypothesis, mostly in the $\pm 20\,\mu$m range, was observed. Taking the shape of the sensors into account removed most of the structure observed in the local-x and local-y residuals. Adding the correct shape into the track reconstruction will possibly help in improving the precise determination of track parameters such as the impact parameter.

References

[1] ATLAS Collaboration, "Measurement of the W-boson mass in pp collisions at $\sqrt{s} = 7\,$TeV with the ATLAS detector," Eur. Phys. J. C **78**, no. 2, 110 (2018) [arXiv:1701.07240 [hep-ex]].

[2] ATLAS Collaboration, "The ATLAS Experiment at the CERN Large Hadron Collider," JINST **3**, S08003 (2008).

[3] ATLAS Collaboration, "Alignment of the ATLAS Inner Detector with the initial LHC data at $\sqrt{s} = 13\,$TeV," ATL-PHYS-PUB-2015-031, https://cds.cern.ch/record/2038139.

[4] ATLAS Collaboration, "Studies of radial distortions of the ATLAS Inner Detector," ATL-PHYS-PUB-2018-003, https://cds.cern.ch/record/2309785.

[5] ATLAS Collaboration, "Operation and performance of the ATLAS semiconductor tracker," JINST **9**, P08009 (2014) [arXiv:1404.7473 [hep-ex]].

[6] ATLAS Collaboration, "ATLAS Insertable B-Layer Technical Design Report," CERN-LHCC-2010-013, ATLAS-TDR-19, https://cds.cern.ch/record/1291633.